Spin-transfer torque efficiency measured using a Permalloy nanobridge

M. C. Hickey,[1,a)] D.-T. Ngo,[2,b)] S. Lepadatu,[1] D. Atkinson,[3] D. McGrouther,[2] S. McVitie,[2] and C. H. Marrows[1,c)]
[1]*School of Physics and Astronomy, University of Leeds, Leeds LS2 9JT, United Kingdom*
[2]*School of Physics and Astronomy, University of Glasgow, Glasgow G12 8QQ, United Kingdom*
[3]*Department of Physics, Durham University, Durham DH1 3LE, United Kingdom*

(Received 16 August 2010; accepted 4 November 2010; published online 19 November 2010)

We report magnetoresistance, focused Kerr effect, and Lorentz microscopy experiments performed on a nanoscale Permalloy bridge connecting microscale pads. These pads can be switched from a parallel to antiparallel state through the application of small fields, causing a detectable magnetoresistance. We show that this switching field H_{sw} is modified by the application of a high current density (J_{dc}) through spin-transfer torque effects, caused by the spin-current interacting with the magnetization gradients generated by the device geometry, yielding an estimate for the spin-transfer torque efficiency $\xi = dH_{sw}/dJ_{dc} = 0.027 \pm 0.001$ Oe/MA cm^{-2}. © *2010 American Institute of Physics*. [doi:10.1063/1.3520144]

It has become a commonplace that spin-polarized currents, flowing through ferromagnets containing magnetization gradients, give rise to spin-transfer torques that act locally on the magnetization.[1,2] The experimentally observed consequences include domain wall (DW) motion,[3–8] depinning,[9–12] resonance,[13–16] and transformation.[17] This effect has applications in solid state storage class memories[18] and is the basis for a magnetic logic gate design.[19]

Here we report on the effects of a spin-polarized current on well-characterized and controlled magnetization gradients that are generated through selection of device geometry. We used a structure based on one originally designed by Jubert *et al.*,[20] where a magnetization gradient is generated in a nanoconstriction that forms a bridge between two microscale pads, which have their shapes chosen to give differing coercive fields. The application of small fields can hence switch the pads into lateral parallel (P) or antiparallel (AP) magnetic states. We subsequently refined that design to give a larger difference in coercivity between the two pads,[21] and measured the magnetoresistance (MR) associated with switching. Here we show that the current density flowing through the bridge affects the switching field as detected by MR, and extract the spin-transfer torque efficiency ξ, defined as the effective magnetic field per unit current density.

The samples were fabricated by either electron beam lithography, sputter deposition of a 7 nm thick Permalloy (Py) layer capped with 2 nm Au, and liftoff, either on thermally oxidized Si substrates, for MR and magneto-optical measurements, or on an electron transparent Si_3N_4 membrane for domain imaging measurements. The bridge connecting the two pads was 300 nm wide and 900 nm long. Ti/Au contacts for transport were added by a further optical lithography liftoff step, and MR measurements were carried out using a standard lock-in detection method. The ac excitation current was $I_{ac} = 50$ μA at 1333 Hz, with a dc bias current I_{dc} added for certain measurements. The geometry is such that high current densities are localized at the bridge. Local magnetometry was carried out using focused magneto-optic Kerr effect (MOKE) measurements, with an elliptical spot size of $\sim 7 \times 5$ μm^2, using a diode laser. Imaging was carried out using Lorentz scanning transmission electron microscopy, with vector maps of the magnetic induction in the region surrounding the bridge obtained by differential phase contrast (DPC) imaging.

In Fig. 1(a) we show our device geometry. The extended shape of the two pads defines a magnetic easy axis. The

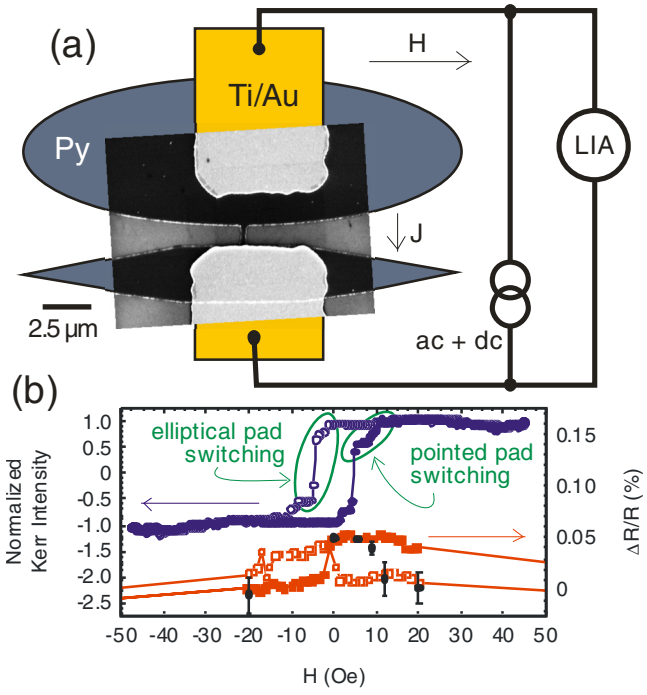

FIG. 1. (Color online) Device geometry and switching. (a) A scanning electron micrograph of a completed device with surrounding schematic showing the full device outline and measurement circuit, with field axis marked. (b) Focused MOKE (circles) and MR (squares) hysteresis loops, with solid symbols for the positive-going field sweep, open symbols for the negative-going sweep. The larger area of the elliptical pad means it yields a larger signal in MOKE. The black solid points (●) are scaled values of $\cos^2\theta$ from the DPC imaging.

[a)]Present address: Department of Physics, University of Massachusetts Lowell, One University Avenue, Lowell, MA 01854, USA.
[b)]Present address: Information Storage Materials Laboratory, Toyota Technological Institute, Nagoya 468-8511, Japan.
[c)]Electronic address: c.h.marrows@leeds.ac.uk.

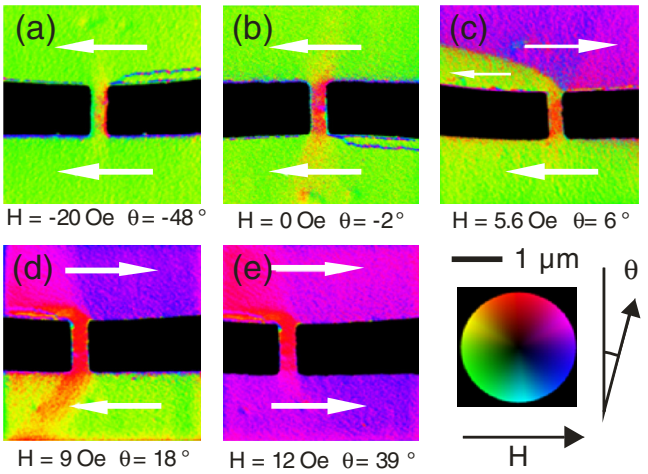

FIG. 2. (Color online) Magnetic induction vector maps constructed from scanning DPC images, which may be interpreted using the color wheel. The soft elliptical pad is uppermost. The average magnetization direction within the bridge is given for each frame along with the value of applied field.

elliptical pad is designed to have a lower switching field than the narrower element,[21] which has pointed ends to increase its coercivity.[22] Conventional current flowing across the bridge from the pointed to the elliptical pad is defined as positive, with electrons flowing in the other direction. The measured device resistance $R \sim 180\ \Omega$.

A focused MOKE hysteresis loop is displayed in Fig. 1(b) for a similar device of this geometry with the laser spot overlapping both pads. We see separate switching events for the two pads, which we confirmed by shifting the laser spot to cover only one or the other. P and AP states for this structure can be defined by analogy to a spin-valve structure, according to whether the magnetization in the two pads is pointing in the same or opposite directions. During a major loop, the AP state occurs between the two switching fields of the pads, and manifests itself as a plateau in the MOKE loop between the switching events, in this case between $H=5.2$ and 8.2 Oe. The MR loop shows magnetic switching from a high to low resistance state as the field is swept, with a subsequent return to a low resistance state at high field (beyond the range of the data shown here). It is noteworthy that the switch into the high resistance state occurs before the field has passed through zero, contrary to our expectation based on the switching into the AP state observed by focused MOKE.

Our magnetotransport measurements are very sensitive to the magnetic state in the region of the bridge. To study this more closely, Lorentz microscopy was carried out on a similar Py nanostructure. The magnetic induction vector maps constructed from DPC images are shown in Fig. 2. The DPC measurement allows the direction of the magnetic induction to be calculated, in the bridge region the average angle of the induction is calculated along with its measured variance. A negatively magnetized P state is shown in panel (a). While the pads are uniformly magnetized in the negative direction, the shape anisotropy in the bridge gives rise to a magnetization texture in its vicinity. Analysis of the DPC image shows that on average the magnetization in the bridge is canted at an angle of $\theta=-48\pm10°$ to the vertical, leading to regions of DW-like rotation of the magnetization at either end, with thicknesses Δ of several tens of nm. The canting away from $\theta=0$ reduces the exchange energy costs in these regions.

The subsequent state at remanence ($H=0$) is shown in panel (b). While the pads remain unswitched, the magnetization in the bridge has relaxed to lie more closely along its axis: now $\theta=-2\pm6°$ and horn-shaped regions of canted magnetization extend from the bridge into the pads. On applying a forward field the magnetization in the softer elliptical pad forms a rippled state (not shown here) and then reverses with a 180° DW sweeping through the ellipse and pinning at the junction with the bridge, shown in panel (c). The magnetization in the bridge remains closely aligned with its axis, with $\theta=+6\pm5°$. On the scale of the Kerr laser spot the system is in the AP state, but these images show that locally the situation is more complex. Upon increasing H further, the DW is depinned from the bridge and the elliptical pad fully reverses, shown in panel (d), and now the magnetization begins to twist away from the bridge axis again, with $\theta=+18\pm6°$. For still higher H the pointed pad reverses, again preceded by a rippled state (not shown), returning the device to a positively magnetized P state, shown in panel (e), with $\theta=+39\pm9°$. At $H=20$ Oe, $\theta=44\pm9°$ (this image is not shown). The values for θ are consistent, within error bars, with those obtained by micromagnetic modeling.[23]

It is known from our previous experiments that MR can be observed due to the magnetic switching of such devices, which arise not from intrinsic DW MR,[24] but are due to the anisotropic magnetoresistance (AMR) effect.[21,25] Most of the resistance arises in the bridge itself, and so this measurement essentially acts as a nanomagnetometer,[26] measuring the local magnetization direction in the bridge. The AMR gives rise to a drop in resistance wherever the magnetization direction is rotated away from collinearity with the current density. We would therefore expect a resistance contribution $\propto\cos^2\theta$. Scaled values of this quantity are overlaid on the MR curve in Fig. 1(b). Consideration of the DPC images shows that it is not strictly the change from P to AP state that controls the MR, but the magnetization angle in and immediately around the bridge: switching into a low θ state occurs before the field passes through zero, consistent with the upward jump in MR observed in Fig. 1(b). While the downward jump is not properly reproduced, it should be noted that we are comparing different samples.

We now turn to the effects of dc current offsets on the MR data, our key experiment in this report. As shown above we can determine the switching field H_{sw} of the bridge from a MR measurement, by first applying a large reverse field (−200 Oe) to saturate the sample into a P state with both pads magnetized in the negative direction, then sweeping it positive and observing at what field we get an abrupt upward step in resistance. In Fig. 3 we show a plot constructed from a series of such normalized MR (Δ) sweeps carried out with different values of negative and positive J_{dc}. The total device resistance was found to rise as J_{dc}^2 due to Joule heating. The bridge resistance rose by $\sim10\ \Omega$ at the highest current densities used. In Fig. 3 we plot the MR ratio $\Delta R/R$ separately normalized for each run, and so this background effect is not evident.

The MR switching field H_{sw} for $J_{dc}=0$ is 1.5 ± 0.5 Oe, corresponding to a change from red to blue contrast in the plot. We can see from Fig. 3 that the effect of a finite value of dc offset current is to shift the observed switching field. The phase boundary for low $R\rightarrow$ high R switching is marked by a dotted black line in Fig. 3, and the switching field is seen to

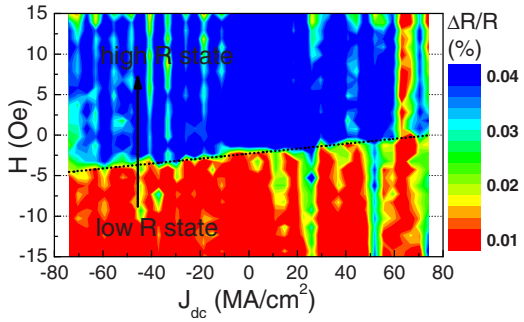

FIG. 3. (Color online) dc current offset effects on the MR. The bitmap is constructed from a series of MR field sweeps carried out for different values of J_{dc}, carried out after reverse saturation. The field sweep direction from low to high R states is shown, and the phase boundary between them is marked with a dotted black line. Small but unavoidable drifts in some of the MR sweeps leads to some vertical streaking in the plot at higher values of J_{dc}.

follow a linear relationship with J_{dc}. This is a signature of spin-transfer torque phenomena, any thermal activation effect would appear even in current. The spin-transfer torque takes effect by displacing some of the magnetization texture at the ends of the bridge.

The rate of change of switching field with current density can be defined as a spin-transfer efficiency, measured here as $\xi = dH_{sw}/dJ_{dc} = 0.027 \pm 0.001$ Oe/MA cm^{-2} from a linear fit to all the switching fields. Although measured by a different method, this is of the same order as that measured for Py by Vernier *et al.*, 0.05 Oe/MA cm^{-2}.[6] As a secondary result, we can estimate from ξ the spin-torque nonadiabaticity parameter from standard theory describing spin-torque at DWs,[27] (related to, but distinct from, the Slonczewski torques in multilayer nanopillars[28]) using the formula $\beta = 2eM_s\Delta\mu_0\xi/P\hbar\pi$.[8] For Py, the magnetization $M_s = 0.83$ MA/m,[29] and polarization $P = 0.5$.[12] Analysis of the DPC images leads to DW widths $\Delta \sim 100$ nm, yielding $\beta \sim 0.04$, the same as previous estimates by us for Py in other depinning studies,[11,12] and approximately five times the Gilbert damping constant $\alpha \approx 0.008$ in our Py films prior to patterning.[30] We note, however, that this formula for β is only valid when the energy barrier to be overcome is linear in H, and we are not certain that this is the case here.[31]

To summarize, we have studied the effect of high current densities on the micromagnetic state of a nanoscale bridge connecting two microscale Py pads by measuring the characteristic AMR signal that indicates switching of the magnetization direction in the bridge. The switching field was found to have a linear dependence on the current density. The canting angle θ is given by equilibrium between the torques exerted on the bridge magnetization that arise from the following energy terms: shape anisotropy, Zeeman, and exchange coupling to the magnetization in the pads. The spin-transfer torque adjusts this equilibrium point, with $J_{dc} > 0$ providing an equivalent negative effective field, delaying the relaxation of the bridge magnetization to point along its length.

This work was carried out under the auspices of the Spin@RT consortium, funded by the EPSRC, Grant Nos. EP/D000661/1 and EP/D062357/1 (Leeds), EP/D003199/1 (Glasgow), and EP/D50578X/1 (Durham), and the European Science Foundation EUROCORES project Spincurrent.

[1] L. Berger, J. Appl. Phys. **55**, 1954 (1984).
[2] C. H. Marrows, Adv. Phys. **54**, 585 (2005).
[3] P. P. Freitas and L. Berger, J. Appl. Phys. **57**, 1266 (1985).
[4] L. Gan, S. H. Chung, K. H. Aschenbach, M. Dreyer, and R. D. Gomez, IEEE Trans. Magn. **36**, 3047 (2000).
[5] J. Grollier, P. Boulenc, V. Cros, A. Hamzić, A. Vaurès, and A. Fert, Appl. Phys. Lett. **83**, 509 (2003).
[6] N. Vernier, D. A. Allwood, D. Atkinson, M. D. Cooke, and R. P. Cowburn, Europhys. Lett. **65**, 526 (2004).
[7] G. Meier, M. Bolte, R. Eiselt, B. Krüger, D.-H. Kim, and P. Fischer, Phys. Rev. Lett. **98**, 187202 (2007).
[8] L. San Emeterio Alvarez, K.-Y. Wang, S. Lepadatu, S. Landi, S. J. Bending, and C. H. Marrows, Phys. Rev. Lett. **104**, 137205 (2010).
[9] C. K. Lim, T. Devolder, C. Chappert, J. Grollier, V. Cros, A. Vaures, A. Fert, and G. Faini, Appl. Phys. Lett. **84**, 2820 (2004).
[10] M. Hayashi, L. Thomas, C. Rettner, R. Moriya, X. Jiang, and S. S. Parkin, Phys. Rev. Lett. **97**, 207205 (2006).
[11] S. Lepadatu, M. C. Hickey, A. Potenza, H. Marchetto, T. R. Charlton, S. Langridge, S. S. Dhesi, and C. H. Marrows, Phys. Rev. B **79**, 094402 (2009).
[12] S. Lepadatu, A. Vanhaverbeke, D. Atkinson, R. Allenspach, and C. H. Marrows, Phys. Rev. Lett. **102**, 127203 (2009).
[13] E. Saitoh, H. Miyajima, T. Yamaoka, and G. Tatara, Nature (London) **432**, 203 (2004).
[14] L. Thomas, M. Hayashi, X. Jiang, R. Moriya, C. Rettner, and S. S. P. Parkin, Nature (London) **443**, 197 (2006).
[15] D. Bedau, M. Kläui, S. Krzyk, U. Rüdiger, G. Faini, and L. Vila, Phys. Rev. Lett. **99**, 146601 (2007).
[16] S. Lepadatu, O. Wessely, A. Vanhaverbeke, R. Allenspach, A. Potenza, H. Marchetto, T. R. Charlton, S. Langridge, S. S. Dhesi, and C. H. Marrows, Phys. Rev. B **81**, 060402 (2010).
[17] M. Kläui, P.-O. Jubert, R. Allenspach, A. Bischof, J. A. C. Bland, G. Faini, U. Rüdiger, C. A. F. Vaz, L. Vila, and C. Vouille, Phys. Rev. Lett. **95**, 026601 (2005).
[18] S. S. P. Parkin, M. Hayashi, and L. Thomas, Science **320**, 190 (2008).
[19] P. Xu, K. Xia, C. Gu, L. Tang, H. Yang, and J. Li, Nat. Nanotechnol. **3**, 97 (2008).
[20] P. O. Jubert, R. Allenspach, and A. Bischof, Phys. Rev. B **69**, 220410 (2004).
[21] M. C. Hickey, D. Atkinson, C. H. Marrows, and B. J. Hickey, J. Appl. Phys. **103**, 07D518 (2008).
[22] K. J. Kirk, J. N. Chapman, S. McVitie, P. R. Aitchison, and C. D. W. Wilkinson, Appl. Phys. Lett. **75**, 3683 (1999).
[23] D. T. Ngo, Ph.D. thesis, University of Glasgow, 2010.
[24] C. H. Marrows and B. C. Dalton, Phys. Rev. Lett. **92**, 097206 (2004).
[25] T. Haug, K. Perzlmaier, and C. H. Back, Phys. Rev. B **79**, 024414 (2009).
[26] K. Hong and N. Giordano, Phys. Rev. B **51**, 9855 (1995).
[27] A. Thiaville, Y. Nakatani, J. Miltat, and Y. Suzuki, Europhys. Lett. **69**, 990 (2005).
[28] J. C. Slonczewski, J. Magn. Magn. Mater. **159**, L1 (1996).
[29] J. M. D. Coey, *Magnetism and Magnetic Materials* (Cambridge University Press, New York, 2010).
[30] S. Lepadatu, J. S. Claydon, C. J. Kinane, T. R. Charlton, S. Langridge, A. Potenza, S. S. Dhesi, P. S. Keatley, R. J. Hicken, B. J. Hickey, and C. H. Marrows, Phys. Rev. B **81**, 020413 (2010).
[31] J.-V. Kim and C. Burrowes, Phys. Rev. B **80**, 214424 (2009).